Lasers in Manufacturing Conference 2023

Surface topology and shape investigation of soda-lime glass structured by ultrashort pulsed laser with long focal length

Sebastian Funken[a,*], Max-Jonathan Kleefoot[a], Christian Neusüß[b], Harald Riegel[a]

[a]*LaserApplicationCenter (LAZ), Aalen University, 73430 Aalen, Germany*
[b]*Department of Chemistry, Aalen University, 73430 Aalen, Germany*

Abstract

In recent years, the use of innovative materials such as glass has become increasingly important, especially to substitute polymers in Lab-on-a-Chip applications. This trend is supported by the growing possibilities of laser material processing with ultrashort pulse lasers. In this work, we present the generation of geometrically defined structures on the surface of soda-lime glass by direct laser ablation as an alternative to laser etching with potassium hydroxide. A femtosecond NIR laser with a long focal length of 100 mm was used. Essential parameter correlations, such as pulse energy to ablation depth or pulse-and-track overlap, were investigated. By using direct laser ablation, the flexibility of scanner-based laser ablation can also be utilized through a depth of approximately 160 µm without refocusing. In this process, a slight ablation depth of roughly 5 micrometers could be achieved, compared to only a few tens of nanometers by the laser-etching process.

Keywords: soda-lime glass; long focal length; structuring; ultrashort pulsed laser; direct writing

1. Introduction

Laser material processing with ultrashort pulse lasers (USP) has established itself as an effective method for precise processing of various materials. Soda-lime glass is also of particular interest in the life science field for microscopy and biotechnology applications because of its easy processability and widespread use (Lin et al., 2001). Overall, USP lasers enable high precision in the fabrication of fine structures or complex shapes in glass, such as microfluidic components (Farson et al., 2008). Thermal damage, through processing, as well as stresses in the glass are minimized for this purpose. The combination of USP lasers together with scanners offers high flexibility in material processing. The use of galvanometer scanners combined with long focal length allows precise and fast deflection of the laser beam in the range of several m/s compared to structuring with microscope optics, where the velocities are in the range of mm/s, used in ablations experiments by Schwarz et al. (Schwarz et al., 2021). Furthermore, high-power ultrashort pulse lasers with high repetition rates are

increasingly used (Thibault et al., 2018). However, thermal accumulation effects can occur when scanning at high repetition rates, especially for glass processing, which can lead to deviations in the shape contour. Another limiting aspect of 2.5D laser material processing by direct laser ablation is the constant need to refocus on the new surface for each layer (Owusu-Ansah et al., 2020). This often results in ablation with low depths (Stonyte et al., 2022). While this may be important for nanostructuring applications with low surface roughness, these parameter windows result in long processing times when fabricating large structures and are impractical for surface structuring of deep geometries. With respect to large structure sizes, it is necessary to optimize process times further, so direct laser ablation remains a preferred method for structuring in this case. For this purpose, we have investigated the two-dimensional ablation behavior in direction of ablation depths in the range up to 10 µm. In this work, we continue to investigate the influence of defocusing at high structure depths with a long focal length. Additionally, a shape deviation based on heat accumulation could be shown using a defined pyramidical 2.5D structure applicable for microfluidic reservoirs.

2. Materials and Methods

The used laser source for the experimental study was a TruMicro 2020 (TRUMPF, Germany), which is integrated into a high-precision machine "microcutUKP" (LLT Applikation GmbH, Germany). The laser emits at 1030 nm and operates at a pulse duration of 350 fs. The average power of the laser is 20 W and the used basic repetition rate is 1000 kHz, resulting in a pulse energy of 20 µJ. The laser beam was focused on the sample using an excelliScan 14 galvo scanner (SCANLAB GmbH, Germany) equipped with a telecentric f-theta lens with 100 mm focal length. The experiments were performed with a focus diameter of 16 µm and a rayleigh length of 210 µm. For laser processing, a sample holder was fabricated to allow glass samples in the form of slides to be easily inserted into the setup (Figure 1). The experimental setup was then attached to the positioning table of the processing unit.

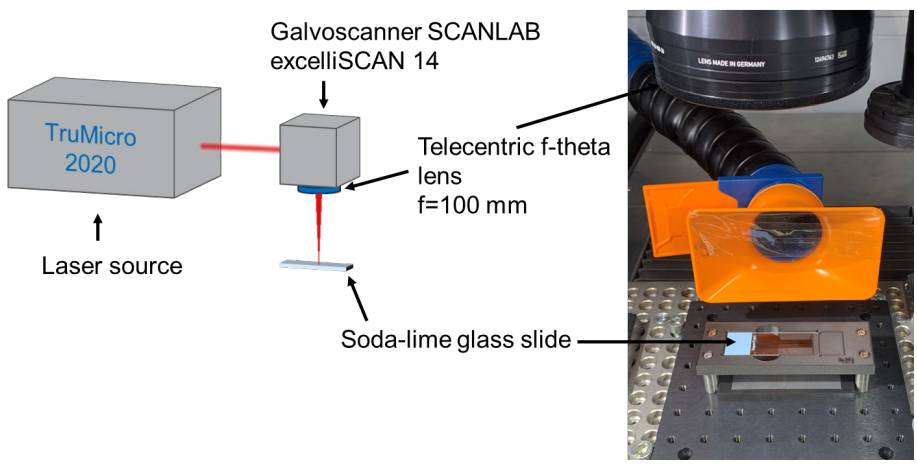

Fig. 1. Experimental setup. Femtosecond laser source TruMicro 2020, galvoscanner for beam deflection and focusing with a telecentric f-theta lens of 100 mm focal length.

The used material was soda-lime glass slides of the brand SuperFrost®. They have the dimensions of 76 mm length, 26 mm width and 1 mm thickness. Focusing was done on the upper surface of the glass. The Z-position adjustment was repeated for each specimen before processing to ensure that the focus was on the surface. The specimens for direct laser ablation were cleaned after processing in a standard ultrasonic basin.

Surface structure and ablation depth analysis was performed using a Zygo NewView 8300 white light interferometer and a Keyence VK-X3050 3D laser scanning confocal microscope.

3. Results and Discussion

First, a two-dimensional surface ablation was investigated by preliminary parameter studies with different pulse and hatch overlaps. The goal was to achieve a uniform but overall shallow ablation depth. The ablation depth with different pulse overlap and hatching can be seen in Figure 2, resulting in homogeneously structured areas within a single scan pass (Figure 3). As a result, a minimum ablation depth of 6 µm and a maximum depth of 15 µm were observed. Higher hatch distances result in stable process windows, while small hatches are limited by possible melt formation due to high heat accumulation.

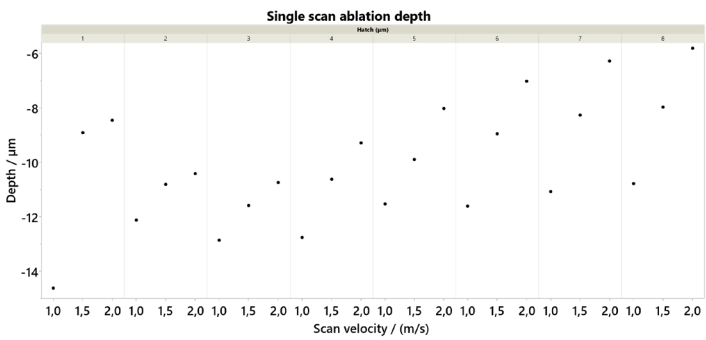

Fig. 2. Preliminary parameter study to determine the single scan ablation depth.

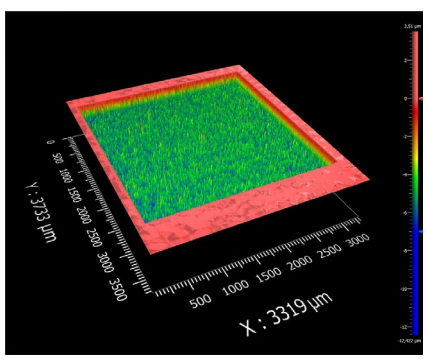

Fig. 3. Pulse energy of 12 µJ, scan velocity of 2 m/s, hatch of 8 µm

To investigate the ablation depth depending on heat input with possible crack formation and in more detail, the same test areas were scanned several times. To also avoid refocusing, four consecutive scans were first performed on a surface with an estimated depth of about 30-40 µm to confirm that the ablation depth per layer is linear within a small defocused range (Figure 4). The initial square size was 8x8 mm^2 and decreased by 2 mm edge length each time to a square of 2x2 mm^2. These tests were performed with a fluence of 6.2 J/cm^2 with a scan velocity of 2 m/s at different hatch distances (5, 6, 7, 8 µm). The average ablation depth per pass ranged from 6.0 µm to 8.4 µm and for the smallest hatch (5 µm) up to a maximum depth of 33.6 µm and showed a linear character throughout (Figure 4). This ablation depth is in accordance with the ablation up to 35 µm shown in the work of Aymerich et al. (Aymerich et al., 2022). However, it appears that the range of linear ablation extends beyond the known range.

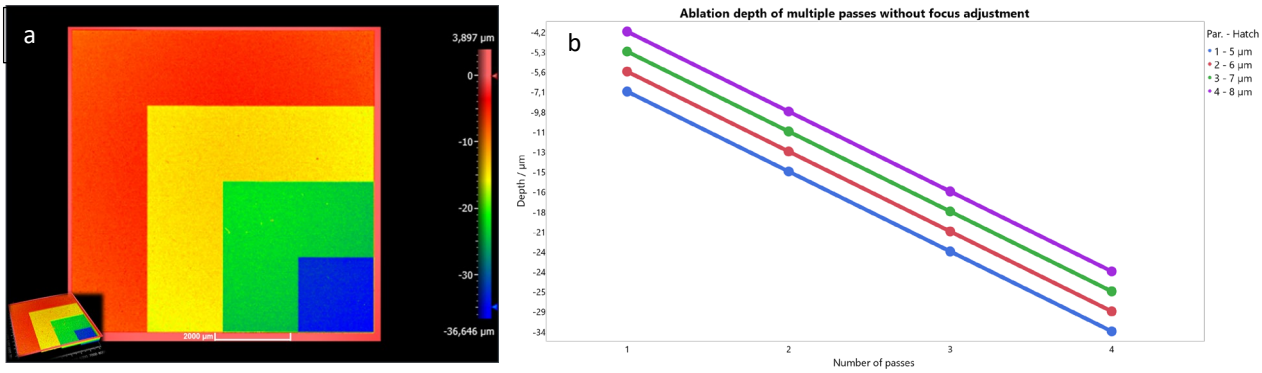

Fig. 4. (a): Surface of ablated area with four scan passes without refocusing. Depth per pass approx. 8 µm. (b) Linear ablation depth of all four hatch parameters with four scan passes.

To investigate the limits of the linear characteristic in more detail, in another experiment, the number of passes was increased to 36 for three different hatches with the same laser parameters. The size of the original square was increased to a 10 mm edge length, which decreased by 200 µm per scan to a minimum area of 3x3 mm^2. To evaluate the process window for linear removal, the removal depth was plotted as a function of the number of scan passes (Figure 5). A linear fit with a correlation of at least 0.9995 was performed. A linear range was observed up to the 18th pass (162.2 µm) for the first field (Hatch:5 µm), up to the 22nd pass (172.2 µm) for the second field (Hatch:6 µm), and up to the 26th pass (168.5 µm) for the third field (Hatch:8 µm). On average, there is a range of 167.7 µm in which the removal is linear and provides a reliable process range for uniform deep structuring. However, in all cases, ablation was observed beyond the rayleigh length of 210 µm. In the first field, a maximum ablation depth of 266 µm was reached in 36 passes, while in fields 2 and 3 the depth reached 250 µm and 217 µm, respectively. The ablation continued to be homogeneous to a Fluence of 2.4 J/cm² across the surface at the 36th pass, but decreased to approximately 40-60 % (3.2 to 4.3 µm) of the initial linear ablation depth for all fields. With these results, a clear range of confidence is opened in which a reproducible ablation can be carried out without refocusing and allows even deeper structuring outside this range with approximate adjustment of the focus.

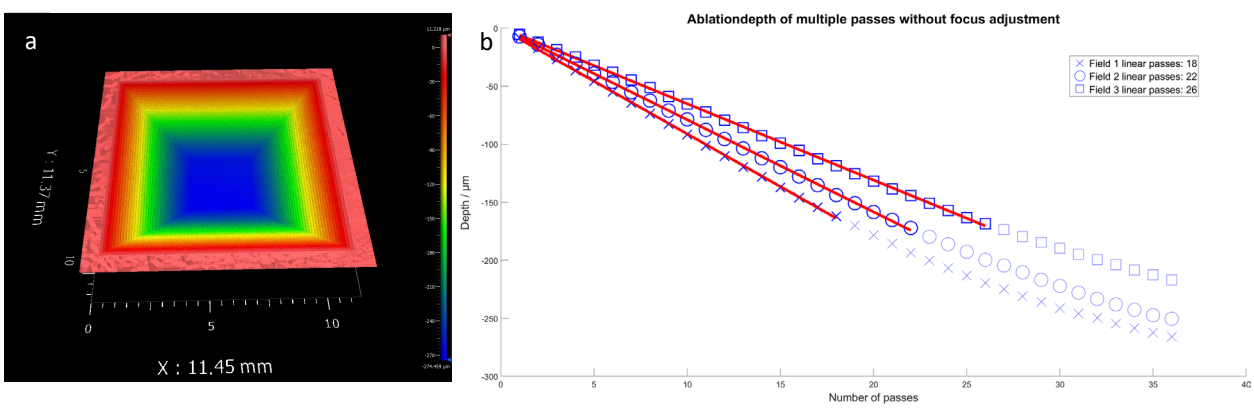

Fig. 5. (a) Structure of 36 consecutive scan passes without refocusing. (b) ablation characteristics for all testes hatch parameters, visible linear ablation up to 167,7 µm and max. ablated depth of 266 µm.

The following 2.5D pyramid was structured accordingly to field 3 from the previous result with a fluence of 6.2 J/cm², scan velocity of 2 m/s, a hatch of 8 µm and a slice of 6 µm. The pyramid should have a base area of 500x500 µm² and a side angle of 30°, corresponding to a depth of 144 µm. The actual base area results in an edge length of 505 µm, the side angle deviates with 37° and results in a depth of 178 µm. Compared to the CAD model in Figure 6, an increase in reduction can be seen as a deviation from the actual shape in the direction of the depth of the structure to the tip of the pyramid. This is potentially due to the small and converging structure by to higher heat accumulation

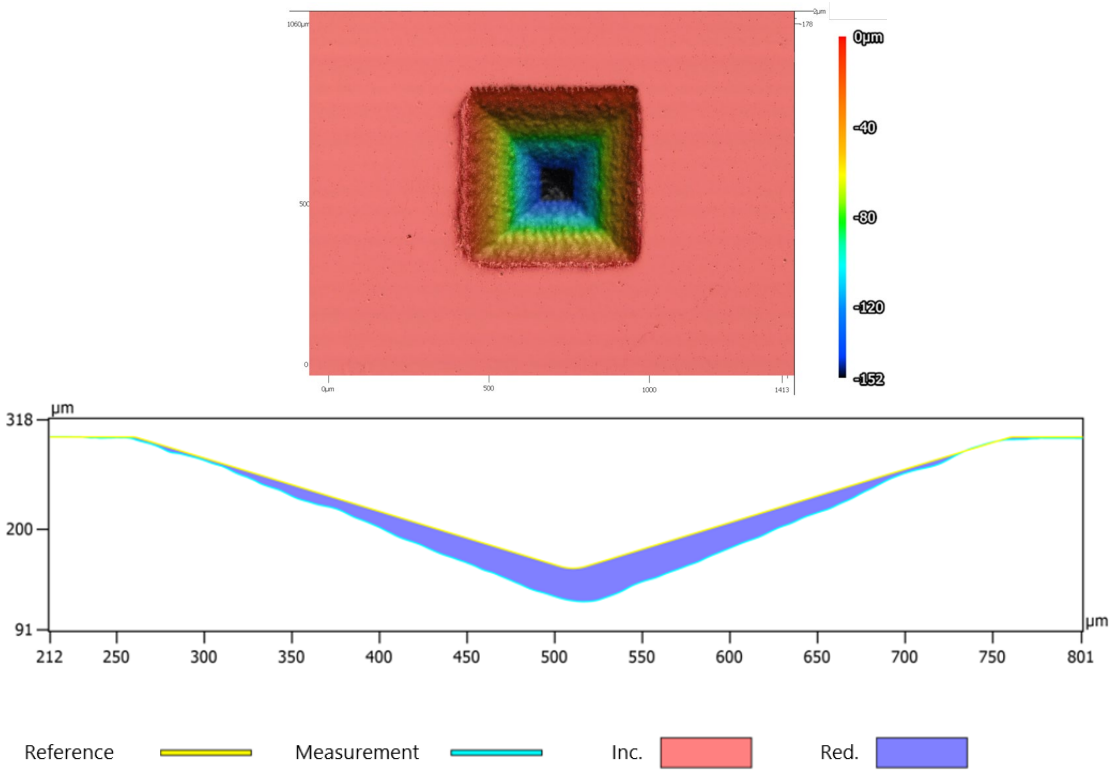

Fig. 6. Comparison between CAD-Model and actual structured geometry. Increasing depth variance towards the tip of the pyramid.

To investigate in more detail the depth increase of the structure, the difference between the CAD model and the measured data of the manufactured pyramid was analyzed. The difference in the Z-direction is shown along the entire centerline of the pyramid. In Figure 7 the behavior can be represented as a Gaussian fit with a correlation R^2 of 0.98, with data in the region of greater structure depth and depth difference ($\Delta > 15$ µm) showing a higher correlation. Toward the center of the structure, the difference increases significantly, corresponding to the difference in the removal rate at this level. This increase reaches its maximum near the top of the pyramid (position 260-270 µm).

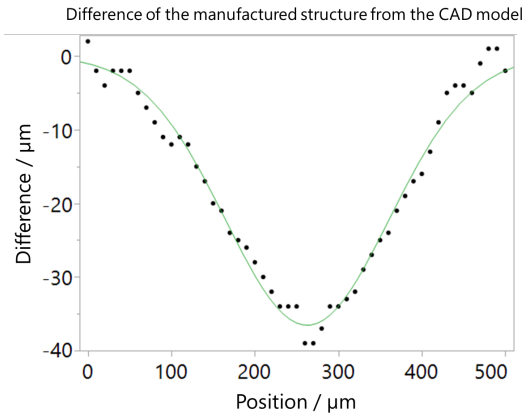

Fig. 7. Increasing difference between CAD-Model and structured geometry. Gaussian increase to the pyramid tip.

A connection can be seen here between the increasingly smaller exposure area with an increase in the approaching structure depth and a stronger influence by heat accumulation. Similarly to the review by Tan et al. (Tan et al. 2021), the heat accumulation needs to be controlled for true shape structuring. In the future, this could be realized with slice-dependent parameters and compensation by adapting the 3D structure model.

4. Conclusion

In this work, we investigated the influence of defocusing at a high structure depth with long focal length of 100 mm without focus adjustment on soda-lime glass, processed with direct laser ablation. At first a linear ablation range of up to 167.7 µm could be observed. The defocused fluence decreased from 6.2 (focal) to 3.8 J/cm². Furthermore, the maximum ablation was up to 266 µm corresponding to a defocused fluence of 2.4 J/cm². In summary, this suggests a lowering of the ablation threshold due to heat accumulation. Additionally, a defined pyramid structure was used to investigate the shape deviation based on heat accumulation as the size of the scan areas decreases in structure depth showing a gaussian-like behavior.
For future research, the influence of geometry-dependent heat accumulation will be investigated in more detail. This also includes possibilities of shape correction by adjusted laser parameters or slice strategies and adjustment of the CAD/CAM-Design for true-to-shape structuring, which is necessary to produce precise microfluidic components with defined volume.

Acknowledgment
The authors acknowledge support by the German Federal Ministry of Education and Research (BMBF), program 'FH-Kooperativ' (ProCEVen, grant no. 13FH135KX0).

References

Aymerich M., Vázquez de Aldana J. R., Canteli D., Molpeceres C., Alvarez E., Almengló C., Flores-Arias M. T., 2022, Soda-lime glass as biocompatible material to fabricate capillary-model devices by laser technologies ,Optical Materials Express, Vol. 12, No. 5, p. 1790

Farson D., Choi H., Zimmerman, Burr S., Jeremy K., Chalmers J., Olesik S.; Lee L., 2008, Femtosecond laser micromachining of dielectric materials for biomedical applications, Journal of Micromechanics and Microengineering,

Lin C., Lee G., Lin Y., Chang G., 2001, A fast prototyping process for fabrication of microfluidic systems on soda-lime glass, Journal of Micromechanics and Microengineering,

Owusu-Ansah E., Dalton C., 2020, Fabrication of a 3D Multi-Depth Reservoir Micromodel in Borosilicate Glass Using Femtosecond Laser Material Processing, Micromachines 2020, 11(12), p. 1082

Schwarz S., Rung S., Esen C., Hellmann R., 2021, Ultrashort pulsed laser backside ablation of fused silica, Optics Express, Vol. 29, No. 15, p. 23477

Stonyte D., Jukna V., and Paipulas D., 2022, Direct Laser Ablation of Glasses with Low Surface Roughness Using Femtosecond UV Laser Pulses, JLMN-Journal of Laser Micro/Nanoengineering Vol. 17, No. 2,

Tan D., Zhang B., Qiu J., 2021. Ultrafast Laser Direct Writing in Glass: Thermal Accumulation Engineering and Applications. Laser Photonics Rev. 2021, 15, 2000455

Thibault F., Haloui H. van Nunen J., 2018, High Repetition Rate USP Lasers Improve OLED Cutting Results, Coherent White Paper